

Human Mitochondrial Thymidine Kinase Is Selectively Inhibited by 3'-Thiourea Derivatives of β -Thymidine: Identification of Residues Crucial for Both Inhibition and Catalytic Activity

Jan Balzarini, Ineke Van Daele, Ana Negri, Nicola Solaroli, Anna Karlsson, Sandra Liekens, Federico Gago, and Serge Van Calenbergh

Rega Institute for Medical Research, Katholieke Universiteit Leuven, Leuven, Belgium (J.B., S.L.); University of Ghent, Ghent, Belgium (I.V.D., S.V.C.); Departamento de Farmacología, Universidad de Alcalá, Alcalá de Henares, Madrid, Spain (A.N., F.G.); and the Karolinska Institute, Huddinge University Hospital, Huddinge, Sweden (N.S., A.K.)

Received November 28, 2008; accepted February 20, 2009

ABSTRACT

Substituted 3'-thiourea derivatives of β -thymidine (dThd) and 5'-thiourea derivatives of α -dThd have been evaluated for their inhibitory activity against recombinant human cytosolic dThd kinase-1 (TK-1), human mitochondrial TK-2, herpes simplex virus type 1 (HSV-1) TK, and varicella-zoster virus TK. Several substituted 3'-thiourea derivatives of β -dThd proved highly inhibitory to and selective for TK-2 (IC_{50} value, 0.15–3.1 μ M). The 3'-C-branched *p*-methylphenyl (compound **1**) and 3-CF₃-4-Cl-phenyl (compound **7**) thiourea derivatives of β -dThd showed competitive inhibition of TK-2 when dThd was used as the variable substrate (K_i values, 0.40 and 0.05 μ M, respectively), but uncompetitive inhibition in the presence of variable concentrations of ATP (K_i values, 15 and 2.0 μ M, respectively). These kinetic properties of compounds **1** and **7** against TK-2 could be accounted for by molecular modeling showing that

two hydrogen bonds can be formed between the thiourea nitrogens of compound **7** and the oxygens of the γ -phosphate of ATP. The importance of several active-site residues was assessed by site-directed mutagenesis experiments on TK-2 and the related HSV-1 TK. The low K_i/K_m ratios for compounds **1** and **7** (0.38 and 0.039 against dThd, and 0.75 and 0.12 against ATP, respectively) indicate that these compounds are among the most potent inhibitors of TK-2 described so far. In addition, a striking close correlation was found between the inhibitory activities of the test compounds against TK-2 and *Mycobacterium tuberculosis* thymidylate kinase that is strongly indicative of close structural and/or functional similarities between both enzymes in relation to their mode of interaction with these nucleoside analog inhibitors.

The important role of mitochondrial nucleoside kinase TK-2 in mitochondrial homeostasis, including maintenance of the mitochondrial dNTP pools and mitochondrial DNA levels, has become increasingly clear in recent years. Mutations in TK-2 have been described in individuals with a mitochondrial DNA depletion syndrome who often develop a devastating myopathy (Saada et al., 2001; Mancuso et al., 2002). In addition, long-term use of some antiviral nucleoside

analogs such as zidovudine, fialuridine, or zalcitabine has been associated with side effects affecting different organs, such as muscle, liver, and/or heart (Lewis et al., 2003; Kohler and Lewis, 2007). It has been suggested that these drug-related toxicities are the consequence of mitochondrial damage due to mitochondrial DNA depletion. This may be caused by long-term inhibition of the TK-2-catalyzed dThd phosphorylation in the mitochondria, which results in thymidine triphosphate depletion (Lynx and McKee, 2006), but also through inhibition of mitochondrial DNA polymerase γ by some of the drugs (Cherrington et al., 1994; Lim and Copeland, 2001). The design and development of specific TK-2 inhibitors may contribute to the study of the role of TK-2 in different physiological processes that can lead to mitochondrial damage (Pérez-Pérez et al., 2008).

A variety of TK-2 inhibitors have been described in the

This work was supported by the Bijzonder Onderzoeksfonds (Universiteit Gent); the Fonds voor Wetenschappelijk Onderzoek (Vlaanderen); the Geconcerteerde Onderzoeksacties Vlaanderen [Grant GOA-05/19]; the Spanish Comisión Interministerial de Ciencia y Tecnología [Grant SAF2006-12713-C02-0]; Comunidad de Madrid [Grants BIPEDD-CM, S-BIO/0214/2006]; and the Swedish Medical Research Council.

Article, publication date, and citation information can be found at <http://molpharm.aspetjournals.org>.
doi:10.1124/mol.108.053785.

ABBREVIATIONS: TK, thymidine kinase; DMSO, dimethyl sulfoxide; HSV, herpes simplex virus; VZV, varicella zoster virus; HPLC, high-performance liquid chromatography; TMPKmt, *Mycobacterium tuberculosis*-encoded thymidylate kinase; dThd, derivative of β -thymidine; CHAPS, 3-[(3-cholamidopropyl)dimethylammonio]propanesulfonate; PBS, phosphate-buffered saline; PDB, Protein Data Bank; MD, molecular dynamics.

literature (Pérez-Pérez et al., 2008) and include 3'-hexanoylamino-dThd (Kierdaszuk et al., 1999), pyrimidine ribofuranosyl nucleosides, 3'-spiroribonucleosides (Balzarini et al., 2000), and arabinosyl nucleosides containing long-chain acyl substituents at the C-2' position of the sugar ring (Balzarini et al., 2001; Manfredini et al., 2001; Ciliberti et al., 2007). It is noteworthy that pyrimidine 2'-deoxynucleoside analogs containing a trityl moiety at the 5'-position of the deoxyribose have also been shown to act as potent and selective inhibitors of TK-2 (Hernández et al., 2002). Further synthetic efforts subsequently led to the identification of and detailed studies on tritylated acyclic pyrimidine nucleoside analogs as TK-2 inhibitors (Hernández et al., 2003). These compounds act as non-nucleosidic inhibitors and are endowed with a pronounced inhibitory activity against the enzyme (50% inhibitory concentrations as low as 0.3 μ M) (Hernández et al., 2002, 2003; Balzarini et al., 2003; Priego et al., 2004; Hernandez et al., 2006; Pérez-Pérez et al., 2008). In this study, we report on the discovery of a series of substituted 3'- or 5'-thiourea derivatives of β - and α -dThd, respectively, as TK-2 inhibitors and the identification of several derivatives that were highly potent in their anti-TK-2 action. This work also revealed the importance of several active-site residues in TK-2 for inhibition and catalytic activity as well as unexpected similarities in inhibitory potency of these inhibitors against the more distantly related mycobacterial thymidylate kinase.

Materials and Methods

Compounds. With the exception of compounds **7** and **8**, the chemical synthesis and characterization of the compounds have been described earlier (Van Daele et al., 2007). For the synthesis of compounds **7** and **8**, 3'-amino-3'-deoxythymidine (100 mg, 0.41 mmol) was dissolved in dimethylformamide (5 ml). After cooling the solution in an ice bath, 1.25 equivalents of the appropriate iso(thio)cyanate was added and the reaction mixture was stirred at room temperature for 3 h. After reaction completion, the reaction mixture was evaporated to dryness, and the residue was purified by column chromatography ($\text{CH}_2\text{Cl}_2/\text{MeOH}$ 95:5 \rightarrow 90:10) to obtain the desired thiourea and urea analogs IVD914 (compound **7**) and IVD918 (compound **8**) in 84 and 81% yields, respectively, as white powders. The following values were obtained for 1-(3'-deoxy-thymidin-3'-yl)-3-(4-chloro-3-(trifluoromethyl)phenyl)thiourea (compound **7**): ^1H NMR (300 MHz, $\text{DMSO}-d_6$): δ 1.79 (3H, d, J = 0.9 Hz, 5- CH_3), 2.16 to 1.2.40 (2H, m, H-2' and H-2''), 3.70 (2H, m, H-5' and H-5''), 3.97 (1H, dd, J = 3.3 Hz and 7.5 Hz, H-3'), 4.84 (1H, m, H-4'), 5.17 (1H, s, 5'-OH), 6.24 (1H, app t, J = 6.6, H-1'), 7.64 (1H, d, J = 8.8 Hz, arom H), 7.72 (1H, dd, J = 2.8 and 9.0 Hz, arom H), 7.80 (1H, s, arom H), 8.09 (1H, d, J = 0.9 Hz, H-6), 8.61 [1H, br s, C(3')NH], 9.78 [1H, br s, C(3')NHC(S)NH], 11.31 [1H, br s, N(3)H]; high-resolution mass spectrometry (electrospray ionization-mass spectrometry) for $\text{C}_{18}\text{H}_{19}\text{ClF}_3\text{N}_4\text{O}_4\text{S}$ [$\text{M}+\text{H}$] $^+$, found, 476.0792; calculated, 479.0762. The following values were obtained for 1-(3'-deoxy-thymidin-3'-yl)-3-(4-chloro-3-(trifluoromethyl)phenyl)thiourea (compound **8**): ^1H NMR (300 MHz, $\text{DMSO}-d_6$): δ 1.79 (3H, d, J = 1.2 Hz, 5- CH_3), 2.12 to 1.2.33 (2H, m, H-2' and H-2''), 3.63 (2H, m, H-5' and H-5''), 3.54 to 3.72 (1H, m, H-3'), 4.29 (1H, m, H-4'), 5.09 (1H, t, J = 5.4 Hz, 5'-OH), 6.19 (1H, app t, J = 6.4, H-1'), 6.89 (1H, d, J = 7.5 Hz, arom H), 7.56 [2H, arom H and C(3')NH], 7.77 (1H, d, J = 1.2 Hz, arom H), 8.07 (1H, d, J = 1.8 Hz, H-6), 8.96 [1H, br s, C(3')NHC(O)NH], 11.29 [1H, br s, N(3)H]; high-resolution mass spectrometry (electrospray ionization-mass spectrometry) for $\text{C}_{18}\text{H}_{19}\text{ClF}_3\text{N}_4\text{O}_4$ [$\text{M}+\text{H}$] $^+$, found, 463.1053; calculated, 463.1040.

Cells. Human lymphocyte CEM cells were cultivated in RPMI 1640 culture medium supplemented with 10% fetal bovine serum, 2 mM L-glutamine, and 0.075% NaHCO_3 . Subcultivations were performed twice a week.

Radiochemicals. The radiolabeled substrate [CH_3 - ^3H]dThd (70 Ci/mmol) was obtained from Moravsek Biochemicals (Brea, CA).

Thymidine Kinase Assay Using [CH_3 - ^3H]dThd as the Natural Substrate. The activity of recombinant thymidine kinase 1 (TK-1), TK-2, herpes simplex virus-1 (HSV-1) TK, and varicella zoster virus (VZV) TK and the 50% inhibitory concentration of the test compounds were assayed in a 50- μ l reaction mixture containing 50 mM Tris/HCl, pH 8.0, 2.5 mM MgCl_2 , 10 mM dithiothreitol, 0.5 mM CHAPS, 3 mg/ml bovine serum albumin, 2.5 mM ATP, 1 μ M [methyl- ^3H]dThd, and enzyme. The samples were incubated at 37°C for 30 min in the presence or absence of different concentrations (5-fold dilutions) of the test compounds. At this time point, the enzyme reaction still proceeded linearly. Aliquots of 45 μ l of the reaction mixtures were spotted on Whatman DE-81 filter paper disks (Whatman, Clifton, NJ). The filters were washed three times for 5 min each in 1 mM ammonium formate, once for 1 min in water, and once for 5 min in ethanol. The radioactivity was determined by scintillation counting.

To determine the K_m (for dThd or ATP) and K_i values (for the inhibitors), varying concentrations of dThd (ranging between 0.4 and 5 μ M) were used at saturating concentrations of ATP (2.5 mM) or varying concentrations of ATP (ranging between 5 and 100 μ M) at saturating concentrations of dThd (20 μ M). The kinetic values were derived from Lineweaver-Burk plots.

Preparation of Murine Liver Homogenates and Stability Measurements of Test Compounds. Seven adult NMRI mice (~20–22 g) were anesthetized with ether, blood was taken by heart puncture, and the mice were subsequently killed by cervical dislocation. Livers were removed and minced with a scissor. The liver pieces were washed twice with ice-cold phosphate-buffered saline (PBS) (6-min centrifugation at 1200 rpm at 4°C) and divided over five tubes (~2 ml each) for homogenization in a Precellys-24 homogenizer using glass beads (Bertin Technol, VWR, Haasrode, Belgium). After homogenization, the suspension was centrifuged for 30 min at 13,000 rpm at 4°C to remove the glass beads and small liver pieces, after which the supernatant was centrifuged again at 25,000 rpm during 2 h at 4°C. Aliquots of this liver extract were then placed in aliquots and frozen at -80°C until use.

Liver extract (200 μ l) was mixed with 200 μ l of PBS and 200 μ l of test compound (300 μ M) to obtain a total volume of 600 μ l (100 μ M test compound). The reaction mixture was incubated for 0, 20, 40, 60, and 240 min at 37°C. At each time point, 100 μ l was withdrawn, added to 200 μ l of ice-cold methanol, centrifuged, and the supernatant analyzed for compound stability by HPLC [Reverse Phase RP-8 (Lichrocard 125-4); Merck, Darmstadt, Germany]. The following gradient was used: 2 min of buffer A (acetonitrile) 2% + buffer B (50 mM NaH_2PO_4 + 5 mM heptane sulfonic acid, pH 3.2); 6-min linear gradient to 20% buffer A + 80% buffer B; 2-min linear gradient to 25% buffer A + 75% buffer B; 2-min linear gradient to 35% buffer A + 65% buffer B; 8-min linear gradient to 50% buffer A + 50% buffer B; 10 min of same buffer mixture; 5-min linear gradient to 2% buffer A + 98% buffer B; and 5-min equilibration at 2% buffer A + 98% buffer B. The compounds **1**, **7**, and **8** had retention times of 20.2, 20.7, and 19.4 min, respectively.

Preparation of Human T-Lymphocyte Extracts and Stability Measurements of Test Compounds. Human T-lymphocyte CEM cells were grown in RPMI 1640 culture medium in a 1-liter culture bottle to a density of 2×10^6 cells/ml. Cells were centrifuged at 1200 rpm at 4°C for 10 min, washed three times with ice-cold PBS, and resuspended in 20 ml of PBS at 100×10^6 cells/ml. After two rounds of 6×20 -s sonication on ice, the cell extract was centrifuged at 13,000 rpm for 30 min at 4°C, and the supernatant was divided in aliquots of 1 ml and frozen at -80°C until use. Stability of the test

compounds was performed as described above for the liver homogenates.

Uptake of Compounds 5 and 8 by CEM Cell Suspensions. A variety of 1-ml suspensions of 10^7 CEM cells in RPMI 1640 culture medium were prepared and exposed to 100 μ M concentrations of compounds 5 and 8. At different time points (15, 30, 45, and 60 min), the cell suspensions were centrifuged and extensively washed (three times) with 1 ml of RPMI 1640 medium (without serum). The cell pellets were then exposed to 66% ice-cold methanol, and the amount of intracellular test compound was determined using HPLC analysis as described above. It was ascertained that any extracellular compound present in the culture medium was efficiently removed because the supernatant after the last centrifugation step did not contain measurable amounts of the compounds.

Model Building and Refinement of Human TK-2. The three-dimensional structure of human TK-2 has not been solved experimentally but a reliable molecular model has been built using a profile-based -fold recognition method (Hernandez et al., 2006). A Mg^{2+} -bound ATP molecule was added to this TK-2 structure, and the complex was further refined by remodeling the loop that closes over the reaction substrates using as a template the X-ray crystal structure of human thymidylate kinase cocrystallized with the inhibitor P^1 -(5'-adenosyl) P^5 -(5'-(3'-azido-3'-deoxythymidyl))pentaphosphate (PDB code 1E9A) (Ostermann et al., 2000).

Docking of a Representative Inhibitor into Human TK-2. The initial geometry for inhibitor 7 was generated using suitable fragments from the X-ray crystal structures of methyl 4-(3-methylphenylureido)-5-methoxymethyltetrahydrofuran-2-carboxylate (code BEQNAN in the Cambridge Structural Database) (Allen, 2002) and dThd as found in the complex with HSV-TK (PDB code 2VTK). The resulting molecular structure was first refined by means of the semiempirical quantum mechanical program MOPAC (Stewart, 1990), using the AM1 Hamiltonian and PRECISE stopping criteria, and further optimized using the restricted Hartree-Fock method and a 6-31G(d) basis set, as implemented in the ab initio program Gaussian 03 (Frisch et al., 2003). The calculated wave function was used to obtain electrostatic potential-derived charges using the restrained electrostatic potential methodology (Bayly et al., 1993).

A multiple structural alignment (Lupyan et al., 2005) of human TK-2, HSV-TK, and human thymidylate kinase provided us with an initial suitable location for both the ATP and the dThd substrates in the active site. The compound 1 inhibitor was placed in the nucleoside binding site of human TK-2 by superimposing the common thymidine skeleton on the docked dThd.

Molecular Dynamics Simulations. The MD simulations were carried out using the AMBER 8.0 suite of programs (Case et al., 2005). The bonded and nonbonded parameters for the compound 1 ligand were assigned, by analogy or through interpolation, from those already present in the AMBER database in a way consistent with the second-generation AMBER force field (Cornell et al., 1995). The molecular system consisting of human TK-2, ATP^{3-} , Mg^{2+} , and compound 1 was neutralized by the addition of five sodium ions (Aqvist, 1990) and immersed in a truncated octahedron of ~6000 TIP3P water molecules (Jorgensen et al., 1983). Periodic boundary conditions were applied, and electrostatic interactions were treated using the smooth particle mesh Ewald method (Darden et al., 1993) with a grid spacing of 1 Å. The cutoff distance for the nonbonded interactions was 9 Å. The SHAKE algorithm (Ryckaert et al., 1977) was applied to all bonds, and an integration step of 2.0 fs was used throughout. First, solvent molecules and counter ions were relaxed by energy minimization and allowed to redistribute around the positionally restrained enzyme-inhibitor complex (25 kcal \cdot mol $^{-1}$ \cdot Å $^{-2}$) during 50 ps of MD at constant temperature (300 K) and pressure (1 atm). These initial harmonic restraints were gradually reduced in a series of progressive energy minimizations until they were completely removed. The resulting system was heated again from 100 to 300 K during 20 ps and then allowed to equilibrate for 500 ps during which positional restraints (5.0 kcal/mol) on the protein C α atoms of

nonloop regions, and distance restraints on the hydrogen bonds between the thymidine moiety and the side chain of Gln110 were used. After this time, the resulting complex was simulated for 10.0 ns in the absence of any ligand restraints, although for the first 3.0 ns, the restraints on the C α atoms of nonloop regions were maintained. System coordinates were collected every 2 ps for further analysis, and the computer graphics program PyMOL (available at <http://www.pymol.org/>) was used for visualization of structures and trajectories.

Model Building and Simulation of the Michaelis-Menten Complex for HSV-1 TK. The three-dimensional X-ray structures of HSV-1 TK in complex with either ADP and deoxythymidine (PDB code 2VTK) or ADP and 5-iodo-deoxyuridine-monophosphate (PDB code 3VTK) (Wild et al., 1997) were used for construction of both the Michaelis-Menten complex with bound ATP^{3-} , an Mg^{2+} ion, and dThd.

To refine the experimental structure, it was necessary to build two missing loops. The Ser149 to Pro153 loop was modeled using as a template the crystal structure of HSV-TK complexed with ganciclovir (PDB code 1KI2, chain B) (Champness et al., 1998). The Gly264 to Pro280 loop was built in two steps: first, the Gly264 to Val267 and Pro274 to Pro280 segments were modeled using as a template the crystal structure of HSV-TK (PDB code 1E2J, chain B) (Vogt et al., 2000); the remaining loop residues (Pro268 to Glu273) were built by the satisfaction of spatial restraints using the MODLOOP server (Fiser and Sali, 2003). The resulting Michaelis-Menten complex was neutralized, immersed in a water bath, equilibrated, and simulated using molecular dynamics for 10 ns in the absence of any restraints.

Site-Directed Mutagenesis, Expression, and Purification of Wild-Type and Mutant Human TK-2. Site-directed mutagenesis of human TK2 was performed using the QuikChange Site-Directed Mutagenesis kit (Stratagene, Heidelberg, Germany). Primers used for Ile59 to His59: 5'-TGTGTCGAGGGCAATCATGCAAGTGGGAAGACG-3' (forward) and 5'-CGTCTTCCCATTGTCATGATTGCCCTCGACACA-3' (reverse); for Ile59 to Leu59: 5'-TGTGTCGAGGGCAATTTAGCAAGTGGGAAGACG-3' (forward) and 5'-CGTCTTCCCATTGCTAAATTGCCCTCGACACA-3' (reverse); for Ile59 to Val59: 5'-TGTGTCGAGGGCAATGTTGCAAGTGGGAAGACG-3' (forward) and 5'-CGTCTTCCCATTGCAACATTGCCCTCGACACA-3' (reverse); for Ile59 to Tyr59: 5'-TGTGTCGAGGGCAATTATGCAAGTGGGAAGACG-3' (forward) and 5'-CGTCTTCCCATTGTCATAATTGCCCTCGACACA-3' (reverse); for Tyr99 to Phe99: 5'-CCTCTGGGCCTGATGTTCCACGATGCCTCT-3' (forward) and 5'-AGAGGCATCGTGGAACATCAGGCCAGAGG-3' (reverse). The human TK2 mutations were verified by sequence determinations of both strands (MWG Biotech, Ebersberg, Germany). We expressed the human TK2 wild-type and mutants in *Escherichia coli* as a fusion protein to glutathione transferase. The plasmids were transformed into Rosetta(DE3) (Novagen, Darmstadt, Germany), and single colonies were inoculated into Luria broth medium supplemented with 100 μ g/ml ampicillin. The bacteria were grown at 37°C, and protein expression was induced at an optical density at 600 nm of approximately 0.8 with 1 mM isopropyl-1-thio- β -D-galacto-pyranoside for ~12 h at 27°C. The expressed protein was purified using glutathione-Sepharose 4B (GE Healthcare, Chalfont St. Giles, Buckinghamshire, UK) as described previously. The purity of the recombinant protein was verified by SDS-polyacrylamide gel electrophoresis (Phast system; GE Healthcare), and the protein concentration was determined with the Bradford Protein Assay (Bio-Rad Laboratories, Hercules, CA) using bovine serum albumin as the concentration standard.

Site-Directed Mutagenesis, Expression, and Purification of Wild-Type and Mutant HSV-1 TK. Mutant HSV-1 TK-enzymes (see Table 2) were derived from the TK sequence cloned in pGEX-5X-1 (Amersham Pharmacia Biotech) (Degrève et al., 2000). Site-directed mutagenesis was performed using the QuikChange Site-Directed Mutagenesis kit (Stratagene) as described before (Fetzer et al., 1994). The two oligonucleotide primers (Invitrogen, Merelbeke,

Belgium) that were used contained the desired mutation at amino acid position 12 and/or 13 of HSV-1 TK. The mutant DNA was transformed into competent *E. coli* XL-1 blue. Plasmid preparations from ampicillin-resistant colonies were checked by sequencing of the TK gene on an ABI Prism 3100 sequencer (Applied Biosystems, Foster City, CA) using the ABI Prism Big Dye Terminator Cycle Sequencing Ready Reaction Kit (Applied Biosystems) and transfected in *E. coli* BL21(DE3)pLysS. Transfected bacteria were grown overnight in 2YT medium containing ampicillin (100 µg/ml) and chloramphenicol (40 µg/ml) and then diluted in fresh medium. After further growth of the bacteria at 27°C (for 5 h), isopropyl-β-D-thiogalactopyranoside (Sigma) was added to a final concentration of 0.1 mM to induce the production of the glutathione transferase-TK fusion proteins. After 16 h of further growth at 27°C, cells were pelleted and resuspended in lysis buffer (50 mM Tris, pH 7.5, 1 mM dithiothreitol, 5 mM EDTA, 10% glycerol, 1% Triton X-100, 0.1 mM phenylmethylsulfonyl fluoride, and 0.15 mg/ml lysozyme) (Göbel et al., 1994). Bacterial suspensions were passed through an SLM Aminco French Pressure Cell Press (Beun de Ronde, La Abcoude, the Netherlands) and ultracentrifuged (20,000 rpm, 4°C, 30 min). Glutathione transferase-TK was purified from the supernatant using Glutathione Sepharose 4B (Amersham) as described by the supplier. The protein content of the purified fractions was assessed using Bradford reagent (Sigma). The following primers were used: for P12N, 5' CGG GTT TAT ATA GAC GGT AAC CAC GGG ATG GGG 3'; for H13I, 5' GTT TAT ATA GAC GGT CCC ATC GGG ATG GGG AAA ACC 3'; for P12N/H13I, 5' CTG CGG GTT TAT ATA GAC GGT AAC ATC GGG ATG GGG AAA ACC 3'. To create the P12N/Y127F, H13I/Y127F and P12N/H13I/Y127F mutant enzymes, DNA of, respectively, the P12N, the H13I, or the P12N/H13I mutants was used instead of wild-type DNA, together with the mutagenesis primers that contain the Y127F mutation.

Results

Inhibition of Pyrimidine Nucleoside Kinases by Substituted 3'- and 5'-dThd Thiourea Analogs. The substituted 3'-branched thiourea-β-dThd and 5'-thiourea-α-dThd derivatives were synthesized and evaluated for their inhibitory activity against dThd phosphorylation by recombinant purified human cytosolic TK-1, human mitochondrial TK-2, HSV-1, TK and VZV TK.

The substituted 3'-branched thiourea-β-dThd derivatives (compounds 1-8) potently inhibited TK-2-catalyzed dThd phosphorylation at IC₅₀ values ranging from 0.43 to 3.1 µM (Table 1). The anti-TK-2 activity was influenced by the nature of the substituent on the

thiourea moiety. The presence of 4-benzyloxyphenyl (4), 4-chloro-3-trifluoromethylphenyl (5), or 3,4-dichlorophenyl (6) moieties on thiourea afforded the best anti-TK-2 activity (Fig. 1 and Table 1). Compounds 4 to 6 showed an outstanding selectivity against TK-2 compared with TK-1 (selectivity index ≥1000). The promising results obtained with derivative 5 prompted us to synthesize 7, in which the similar substituted thiourea group is connected directly to the sugar ring (Fig. 1). Such 3'-amino-3'-deoxythymidine derivatives are synthetically more readily accessible than the branched-chain analogs. Surprisingly, with an IC₅₀ value of 0.15 µM, analog 7 surpassed the inhibitory activity of its branched-chain congener 5, whereas the corresponding urea derivative in which the sulfur atom was replaced by an oxygen (8) proved to be only slightly less inhibitory against the TK-2 enzyme (Table 1). In contrast, all 3'-thiourea-β-dThd analogs (with or without branching) were devoid of inhibitory activity against cytosolic TK-1 at 500 µM; that is, at concentrations that are at least 2 to 3 orders of magnitude higher than those required for TK-2 inhibition. In addition, they showed poor, if any, inhibitory activity against HSV-1 TK (IC₅₀ value, 46 to ≥500 µM) and only moderate activity against the closely related VZV TK (IC₅₀ value, 15–77 µM) (Table 1). Thus, the 3'-branched thiourea-β-dThd analogs showed a surprising specificity for TK-2 compared with HSV-1 and VZV TK that belong to the same family of enzymes, as well as with the more distantly related TK-1.

The corresponding substituted 5'-thiourea-α-dThd derivatives (10-16) were markedly less inhibitory to TK-2 than the substituted 3'-thiourea-β-dThd analogs and completely inactive against TK-1 (Table 1). The most potent inhibitors showed an IC₅₀ value that ranged between 31 and 57 µM, that is, at least 10- to 100-fold less inhibitory than the 3'-thiourea-β-dThd derivatives. They also showed a moderate inhibition of HSV-1 and VZV TK enzymes. The α-dThd lacking the thiourea group at the 5'-position of the deoxyribose, and thus containing free OH groups at the 3' and 5' positions, had an IC₅₀ between 34 and 99 µM for the investigated nucleoside kinases. Taken together, it is clearly seen that the introduction of selected arylthiourea substituents consistently confers TK-2/TK-1 selectivity.

Stability Measurements of Compounds 5, 7, and 8 and Uptake into Human T-Lymphocyte CEM Cells. Compounds 5, 7, and 8 were examined for their stability in human T-lymphocyte CEM cell extracts and in mouse liver homogenates. It was found that the compounds (examined at 100 µM) were fully stable in both CEM cell extracts and mouse liver homogenates when incubated for 20, 40, 60, and

TABLE 1

Inhibitory activity of 3'- and 5'-thiourea derivatives of thymidine against nucleoside kinase-catalyzed phosphorylation of 1 µM [CH₃-³H]thymidine. IC₅₀ is the 50% inhibitory concentration of the test compounds required to inhibit 1 µM [CH₃-³H]dThd phosphorylation by 50%. Data are the mean of two to three independent experiments.

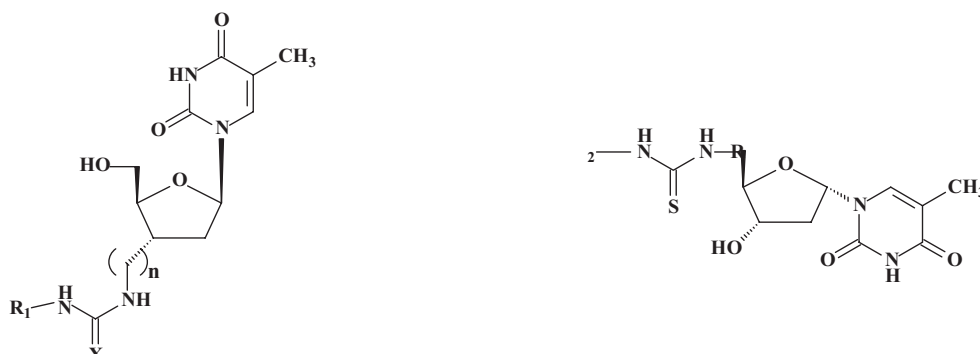
Compound	IC ₅₀			
	TK-1	TK-2	HSV-1 TK	VZV TK
			µM	
1	>500	1.2 ± 0.1	444 ± 18	37 ± 2.0
2	>500	3.1 ± 0.3	≥500	77 ± 51
3	>500	1.2 ± 1.1	400 ± 54	31 ± 5.0
4	≥500	0.43 ± 0.04	232 ± 39	28 ± 1.0
5	≥500	0.47 ± 0.04	46 ± 4.0	21 ± 5.0
6	≥500	0.64 ± 0.31	87 ± 36	15 ± 1.0
7	316 ± 1.2	0.15 ± 0.01	195 ± 54	24 ± 3.0
8	416 ± 6.0	0.42 ± 0.0	335 ± 25	5.6 ± 0.8
9 (α-dThd)	99 ± 51	46 ± 2.0	34 ± 3.0	47 ± 3.0
10	>500	57 ± 20	422 ± 6.0	30 ± 7.0
11	>500	405 ± 78	>500	40 ± 3.0
12	>500	41 ± 3.0	365 ± 22	45 ± 6.0
13	>500	38 ± 1.0	472 ± 40	40 ± 4.0
14	>500	110 ± 13	>500	95 ± 66
15	>500	99 ± 36	>500	150 ± 38
16	>500	31 ± 6.0	392 ± 8.0	45 ± 1.0

240 min at 37°C. No traces of breakdown products could be detected by HPLC analysis of the incubated samples.

Uptake of the test compounds by intact CEM cells was also investigated for compounds **5** and **8**. A comparable and extensive uptake of **5** and **8** by the CEM cells was observed within 15 min (Fig. 2), after which further cellular uptake leveled off. The efficient uptake of the compounds may be related to their (calculated) lipophilic properties (log*P* rang-

ing between 0.92 and 3.08 using Crippen's fragmentation; Ghose and Crippen, 1987) and between 1.34 and 3.77 using Viswanadhan fragmentation (Viswanadhan et al., 1989).

Kinetic Properties of 1 and 7 against TK-2. The mode of inhibitory activity of **1** and **7** against TK-2 was investigated. First, the K_i value for each compound was determined in the presence of a fixed saturating concentration of ATP and variable concentrations of the dThd substrate. Com-



The figure shows the chemical structure of a general dThd 3'-thiourea derivative and the dThd molecule. The derivative has a 2-methyl-4-oxo-1,2,3,4-tetrahydropyrimidin-5-yl group at the 3' position of a deoxyribose sugar, which is linked via a thiourea group (-NH-C(=S)-NH-) to an R1 group. The sugar also has a hydroxyl group at the 2' position and a hydroxymethyl group at the 4' position. The dThd molecule is 2-deoxy-2-thiothymidine, which has a 2-methyl-4-oxo-1,2,3,4-tetrahydropyrimidin-5-yl group at the 3' position of a deoxyribose sugar, which is linked via a thiourea group (-NH-C(=S)-NH-) to a 2-deoxy-2-thiothymine base.

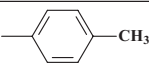
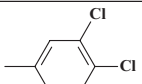
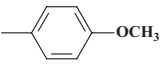
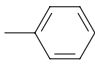
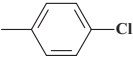
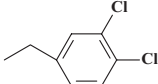
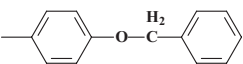
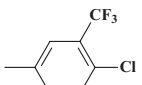
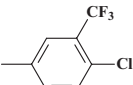
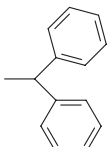
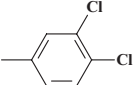
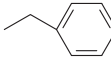
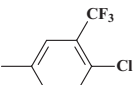
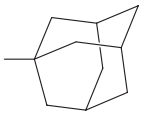
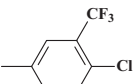
Compound code	X	n	R1	IC ₅₀ (μM) for TK-2	Compound code	R2	IC ₅₀ (μM) for TK-2
1	S	1		1.2	10		57
2	S	1		3.1	11		405
3	S	1		1.2	12		41
4	S	1		0.43	13		38
5	S	1		0.47	14		110
6	S	1		0.64	15		99
7	S	0		0.15	16		31
8	O	0		0.42			

Fig. 1. Structural formulae of TK-2 inhibitors and the 50% inhibitory concentration values for TK-2 using dThd as the substrate.

pounds **1** and **7** inhibited the enzyme in a purely competitive fashion and had K_i values as low as 0.40 and 0.054 μM , respectively (Fig. 3). Their K_i/K_m values were markedly lower than 1 (0.38 and 0.039, respectively), pointing to an affinity for the enzyme that largely exceeds the affinity for the natural substrate. Second, the K_i values of the TK-2 inhibitors were determined in the presence of a fixed saturating concentration of dThd and variable concentrations of the cosubstrate ATP. Compounds **1** and **7** showed K_i values that were higher (1.5 and 2 μM , respectively) than those observed in the presence of dThd as the variable substrate. The K_i/K_m values were again lower than 1 (0.75 and 0.12 μM) (Fig. 3). However, under these conditions, the TK-2 inhibitors behaved kinetically differently and displayed an uncompetitive mechanism of enzyme inhibition, as revealed by the (virtually) parallel kinetic lines in the Lineweaver-Burk plots (Fig. 3). It would also have been interesting to reveal whether compounds **1** and **7** showed uncompetitive kinetics against HSV-1 TK as well in the presence of varying ATP concentrations. However, because of the markedly lower (100- to 1000-fold) inhibitory activity of these compounds against HSV-1 TK, and their limited solubility at concentrations greater than 500 μM , it was impossible to perform these experiments.

Molecular Modeling and Computer Simulations. On the basis of the experimental results, binding of the most potent inhibitor, **7**, to human TK-2 was simulated in the presence of bound ATP. The crucial interactions observed after docking were maintained in the equilibrated complex, and some others ensued from the mutual adaptation brought about by the MD procedure. In the final structure (Fig. 4), the **7** ligand seems to be stabilized in the binding site by the following interactions: 1) the thymine moiety of the inhibitor is sandwiched between the phenyl ring of Phe143 on one side and the side chains of both Trp86 and Val115 on the other side; 2) the thymine O4 and N3 atoms establish good hydrogen bonds with the carboxamide group of Gln110; 3) the O5' hydroxyl is fixed by the guanidinium nitrogen of Arg134; 4) the substituted phenyl ring stacks against the side chain of Ile59 and is oriented such that its trifluoromethyl group

points to Arg196 and the chlorine atom faces a hydrophobic cavity lined by the side chains of Leu193, Ile204, and Leu209; and finally 5) both thiourea nitrogens hydrogen bond to the γ -phosphate oxygens of ATP (Fig. 4).

Construction of Mutant TK-2 and Herpes Simplex Virus Type 1 TK and Susceptibility to the Inhibitory Activity of **1 and **7**.** Our molecular modeling data suggested that the side chain of Ile59 in TK-2 stacks against the phenyl ring of **7**. Because the equivalent position in HSV-1 TK and VZV TK, which are much less sensitive to the inhibitors (Table 1), is occupied, respectively, by either a histidine or a tyrosine (Fig. 5), it was then hypothesized that replacement of Ile59 by any of these more polar amino acids, and also by the slightly different but equally hydrophobic valine and leucine, should have an influence on the potency of the inhibitors against TK-2. Consistent with this view, the conservative I59V and I59L TK-2 mutants showed at least an equal or even a slightly higher (2-fold) sensitivity to the inhibitory activity of **7** and **1** than did wild-type TK-2 enzyme (Table 2). In contrast, the I59H and I59Y TK-2 mutants lost 2- to 3-fold and ≥ 10 -fold sensitivity, respectively, to the inhibitory activity of both test compounds (Table 2). Rather unexpectedly, however, it was also noted that these mutations were considerably damaging (I59V and I59L) or highly detrimental (I59H and I59Y) for the catalytic activity of the mutant TK-2 enzymes, which was decreased to $\sim 15\%$ or $\leq 0.05\%$, respectively, that of the wild-type enzyme. The K_m values for the natural substrate were virtually unchanged (3.9–6.0 μM).

In view of these results, we decided to try a reverse approach aimed at increasing the sensitivity to these inhibitors of the more resilient HSV-1 TK. This enzyme has been structurally characterized in atomic detail by X-ray crystallography in complex with a variety of ligands (Wild et al., 1997; Champness et al., 1998) (PyMOL version 0.99). To this end, the histidine residue (His13) in HSV-1 TK that occupies a position equivalent to that of Ile59 in TK-2 (Fig. 5) was mutated to isoleucine. The H13I HSV-1 TK mutant enzyme turned out to be catalytically virtually inactive and was not inhibited by **7** (Table 2). Because we believed that this outcome could be due to structural rearrangements in the ATP-binding glycine-rich loop that would prevent productive binding of the ATP cosubstrate, we probed the effect of replacing the preceding residue (Pro12) with an asparagine, which is the amino acid present in TK-2 in the equivalent position (Asn58) and does not seem to interact directly with the inhibitor according to our model (Fig. 4). The P12N mutant HSV-1 TK retained $\sim 10\%$ of the catalytic activity of the wild-type enzyme, and both enzymes were inhibited by **7** to a similarly low extent. The additional introduction of this second mutation into the first inactive H13I mutant resulted in a further decrease of the catalytic activity (Table 2). Compound **7** was as poor an inhibitor for the H13I/P12N double mutant as it was for the wild-type enzyme. A new attempt to regain activity in the H13I mutant HSV-1 TK consisted of introducing another second mutation at the position of the residue that most closely interacts with the side chain of this amino acid, that is, Tyr127, which is positionally equivalent to Phe144 in TK-2. The H13I/Y127F double mutant was active because of improved V_{max} and K_m values relative to the single H13I mutant but was still poorly inhibited by **7**. Both the P12N/Y127F double mutant and the H13I/P12N/Y127F triple mutant were catalytically virtually inactive and

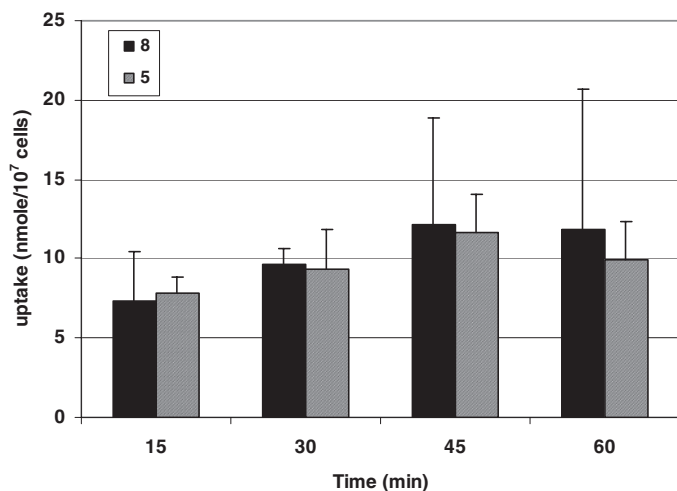


Fig. 2. Uptake of compounds **5** and **8** by T-lymphocyte CEM cells. CEM cell suspensions were exposed to 100 μM test compound, and uptake of compound into the cells at different time points was measured after centrifugation and extensive washing of the cells to remove extracellular compound.

completely resilient to inhibition by the test compounds (Table 2).

Discussion

We report here on a novel structural class of compounds that exert a potent inhibitory effect on mitochondrial TK-2. The most potent and selective compound (i.e., **7**) showed a 2000-fold TK-2 selectivity compared with cytosolic TK-1, against which it was only marginally inhibitory. Compound **7** is the most potent inhibitor of TK-2, with a K_i value of 0.054 μM and K_i/K_m ratio of 0.039 when determined against dThd as the natural substrate. Whereas these compounds were found to display purely competitive inhibition kinetics with respect to dThd, the inhibitors showed an uncompetitive kinetic profile against ATP (K_i/K_m ratio of 0.12 for **7**). In this respect, this class of compounds behaves differently from (*E*)-5-(2-bromovinyl)-2'-deoxyuridine, which showed competitive inhibition against dThd but noncompetitive inhibition against the cosubstrate ATP (Balzarini et al., 2003). Thus, the TK-2 inhibitors herein described most likely occupy (at least partially) the substrate-binding site but only after the cosubstrate ATP is bound to the enzyme. In agreement with this line of reasoning, our molecular model revealed a binding mode whose most intriguing feature is the existence of two hydrogen bonds between the thiourea moiety of the **7** inhibitor and the γ -phosphate of ATP. This finding could

account for the observed unusual kinetic behavior of this type of compounds against the enzyme. It is noteworthy that the substituted thiourea dThd analogs kinetically behave like the acyclic 5'-trityl nucleoside analogs earlier described as TK-2 inhibitors (Balzarini et al., 2003; Hernandez et al., 2006). Indeed, TK-2 inhibition by such inhibitors [i.e., (*E*)-5-(2-bromovinyl)-1-[(*Z*)-4-triphenylmethoxy-2-butenyl]uracil and 1-[(*Z*)-6-pyridyldiphenylmethoxy]hexyl]thymine] is also competitive with respect to dThd but uncompetitive with respect to ATP. A rationale for these kinetic data was provided by docking some of the representative inhibitors into a homology-based model of TK-2 (Hernandez et al., 2006). Our current molecular model can also account for the finding that the 3'-thiourea β -dThd analogs were consistently found to be markedly more inhibitory to TK-2 than the 5'-thiourea α -dThd congeners. Clearly, subtle differences in the orientation of the deoxyribose part seem to have a pronounced effect on the eventual affinity and inhibitory activity against TK-2.

Given the high nucleoside kinase selectivity of the reported inhibitors toward TK-2, we attempted to gain insight into the active site amino acids most likely involved in ligand binding by following two alternative and complementary approaches. On the one hand, we mutated Ile59 in TK-2 to several other amino acids (histidine, tyrosine, valine, and leucine), and on the other hand, we tried to incorporate mutations into HSV-1 TK that would make this enzyme more sensitive to inhibition

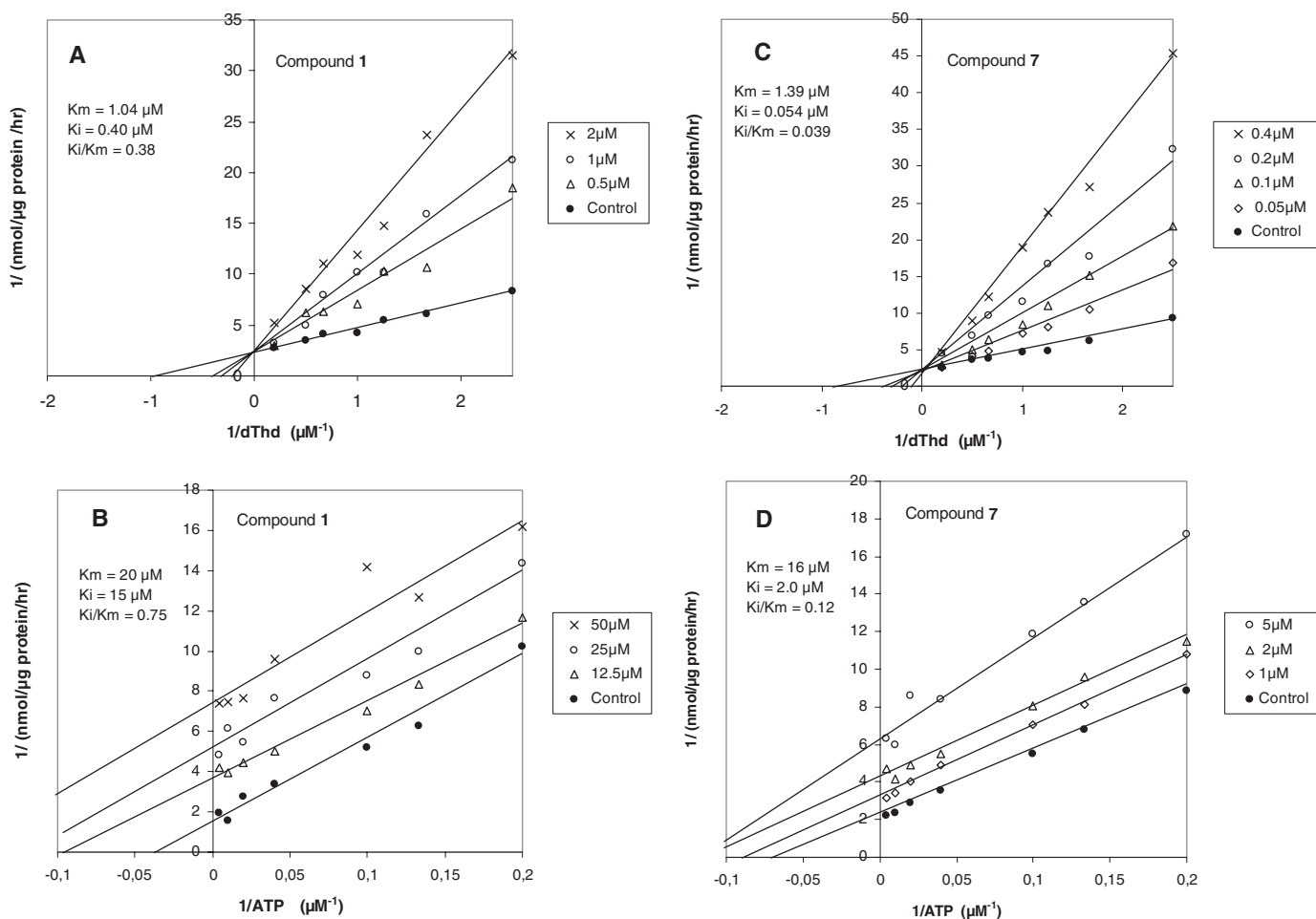


Fig. 3. Kinetics of **1** and **7** against purified recombinant mitochondrial TK-2. Lineweaver-Burk plots (1/substrate versus 1/velocity) are shown for the inhibition of TK-2 by compound **1** (A and B) and compound **7** (C and D) against dThd (A and C) and ATP (B and D) as the competing substrate.

by these TK-2-selective compounds. Because the molecular modeling results pinpointed a hydrophobic stacking interaction between the substituted phenyl ring of **7** and the side

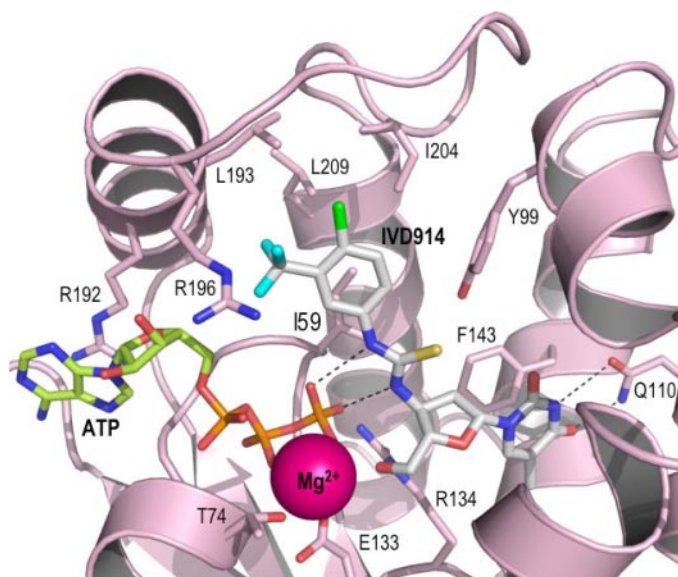


Fig. 4. Proposed binding mode for the best inhibitor, **7** (designated IVD 914) (carbon atoms shown in white), in the active site of human TK-2 (pink ribbon). ATP is shown as sticks, with carbon atoms colored in olive green, and Mg^{2+} is displayed as a sphere colored in magenta. Note the “open” conformation of the loop that normally closes over the reaction substrates. Protein side chains relevant to the discussion are labeled and shown as sticks except for those of Trp86 and Val115, which have been omitted to improve clarity. Broken lines represent hydrogen bonds between the thiourea nitrogens and the oxygens of the γ -phosphate of ATP and between the amide of Gln110 and thymine.

chain of Ile59, we expected weakened ligand binding and partial loss of inhibition for the I59H (as in HSV-1 TK) and I59Y (as in VZV TK) mutant enzymes and no significant differences for the enzymes harboring the more conservative I59V and I59L mutations. Consistent with this reasoning, the latter mutants were similarly or slightly better inhibited by both **7** and **1**, whereas the I59H and I59Y mutant enzymes were less inhibited than wild-type TK-2 (Table 2). What we did not anticipate, however, was the rather drastic loss of catalytic activity that was detected when the kinetic properties of wild-type and mutant enzymes were compared (Table 2).

On the other hand, attempts to make the closely related HSV-1 TK more susceptible to the inhibitory effects of the TK-2-selective compounds by replacing amino acids Pro12 and His13 (X-ray numbering for HSV-1 TK) with their positionally equivalent counterparts in TK-2 (Asn[58] and Ile[59], respectively) were unsuccessful. Furthermore, the catalytic activity of both P12N and H13I mutant enzymes was seriously compromised, particularly in the latter case. When we modeled the Michaelis-Menten complex of the reaction catalyzed by HSV-1 TK we realized that N δ of His13 forms a good hydrogen bond with the hydroxyl group of Tyr127, which is attached to the phenyl ring that provides the stacking interaction to the pyrimidine ring of dThd in the substrate-binding pocket (Fig. 6). It is noteworthy that the equivalent residue in TK-2 is a phenylalanine (Phe144), which cannot form such hydrogen bond, but in this enzyme, the position of His13 is occupied by Ile59, whose side chain can establish a hydrophobic interaction with the phenyl ring of Phe144, according to our model. Because this could be an example of a correlated mutation (Fetzer et al., 1994) we

	55	59						65			140				144				150							
TK-2	...	V	E	G N I A S G						K	T	T	...	A	R	Y	I	F		V	E	N	L	Y	R	...
HSV-1 TK		I	D	G P H G M G						K	T	T		A	L	L	C	Y		P	A	A	R	Y	L	
VZV TK		L	D	G A Y G I G						K	T	T		S	T	I	C	F		P	L	S	R	Y	L	
TK-1		I	L	G P M F S G						K	S	T		F	Q	R	K	P		F	G	A	I	-	-	

Fig. 5. Alignment of the 55 to 65 amino acid stretch in TK-2, HSV-1 TK, VZV TK, and TK-1. The amino acids that were mutated in TK-2 and HSV-1 TK are indicated in boldface type.

TABLE 2

Kinetic parameters for and inhibitory activity of test compounds against wild-type and mutant TK-2 and HSV-1 TK

IC₅₀ is the 50% inhibitory concentration required to inhibit enzyme-catalyzed dThd (1 μ M) phosphorylation by 50%. Data are the mean of two (for TK-2) or two to three (for HSV-1 TK) independent experiments.

	IC ₅₀		K_m (dThd)	V_{max}	V_{max}/K_m
	Compound 1	Compound 7			
	μ M	μ M	μ M	pmol/ μ g/h	
TK-2					
Wild type	1.3 \pm 0.59	0.15 \pm 0.06	4.3 \pm 2.3	1956 \pm 448	455
I59V	0.61 \pm 0.04	0.078 \pm 0.011	5.1 \pm 1.8	328 \pm 59	64
I59L	1.4 \pm 0.75	0.074 \pm 0.007	5.6 \pm 5.0	322 \pm 110	57
I59H	6.1 \pm 2.0	0.31 \pm 0.01	6.0 \pm 2.4	1.2 \pm 0.0	0.20
I59Y	>10	1.8 \pm 0.50	3.9 \pm 2.4	0.60 \pm 0.05	0.15
HSV-1 TK					
Wild type	>100	83 \pm 11	0.44 \pm 0.17	25,667 \pm 13,577	58,334
P12N	>100	57 \pm 23	3.9 \pm 1.3	3000 \pm 424	769
H13I	>100	>100	612 \pm 78	607 \pm 26	0.99
P12N + H13I	>100	72 \pm 40	0.23 \pm 0.042	25 \pm 2.1	109
P12N/Y127F	>100	>100	590 \pm 581	490 \pm 250	0.83
H13I/Tyr127F	>100	87 \pm 9.2	37 \pm 23	1389 \pm 393	37
P12N/H13I/Y127F	>100	>100	263 \pm 194	32 \pm 14	0.12

believed that the catalytic activity of the H13I mutant enzyme would be recovered upon incorporation of a second mutation so as to replace the favorable hydrogen-bonding interaction involving the original His13/Tyr127 couple with an equally favorable hydrophobic interaction between the isoleucine and a phenylalanine, as in the Ile59/Phe144 couple in TK-2 (Fig. 5). This strategy led to an Ile13/Phe127 HSV-1 TK double mutant that was more catalytically active than the single mutants but still more than 1 order of magnitude less active than wild-type HSV-1 TK (Table 2) and not better inhibited by either **7** or **1**. In view of these results, we tend to think that these mutations preclude proper binding of the ATP molecule, and this in turn hampers optimal binding of the inhibitors.

An interesting feature of these thiourea-substituted dThd derivatives is that some of them have recently been reported to inhibit the *Mycobacterium tuberculosis*-encoded thymidylate kinase (TMPKmt) (Van Daele et al., 2007). Nonetheless, whereas the 3'-branched thiourea- β -dThd derivatives were superior to the 5'-thiourea- α -dThd derivatives as TK-2 inhibitors, the opposite was true for *M. tuberculosis* TMPK, for which the 5'-thiourea- α -dThd analogs were the most active inhibitors (Van Daele et al., 2007). It is intriguing that, despite the fact that both enzymes seem to prefer different anomeric configurations of dThd, there is a close correlation between the ranking of the inhibitory potency of these compounds against both enzymes ($r = 0.89$) (Fig. 7). These striking observations may imply that TK-2 and mycobacterial TMPK may be quite similar in terms of interaction kinetics and recognition of modified nucleoside analog inhibitors at the dThd (in TK-2) and thymidylate (in TMPKmt) binding sites. In fact, close structural similarities between TK-2 and TMPKmt have been reported recently (Negri et al., 2007) that were rather unexpected in view of the relatively low sequence identity between these enzymes. This structural similarity would account for the unexpected similar susceptibility to several classes of inhibitors and strongly suggests that broader screening assays may be necessary when pursuing high selectivity.

It should be mentioned that the mitochondria represent cellular organelles that are believed to result from pro-

karyotes that started to live in symbiosis within eukaryotic cells. TK-2 may thus be considered as a prokaryotic-like enzyme similar to the TMPK of *M. tuberculosis*. It would therefore be interesting to expand the inhibition studies with these kind of TK-2 inhibitors to other nucleoside or nucleotide kinases of prokaryotic/parasitic origin. Conversely, some acyclic thymidine nucleoside analogs recently reported as potent inhibitors of *M. tuberculosis* thymidylate kinase (Familiar et al., 2008) should also be evaluated for their inhibitory potential against TK-2. In fact, it is tempting to speculate that the closely similar kinetic behavior in relation to varying concentrations of either dThd or ATP reported for some 5'-tritylated (a)cyclic-dThd analogs described earlier (Balzarini et al., 2003), and the substituted 3'-thiourea β -dThd analogs delineated herein may reflect a similar mode of interaction with TK-2. It is indeed plausible that the lipophilic trityl group in the 5'-trityl β -dThd analogs and the lipophilic substituted phenyl group present on the thiourea moiety of 3'-thiourea β -dThd derivatives may interact with the same binding site on TK-2. It would thus be very interesting to compare structure-activity data for both groups of compounds against TK-2, to try to cocrystallize one or more representative compounds with TK-2, and/or to carry out comparative docking experiments. Efforts in these directions are already under way. In addition, in-depth cell culture studies should also be performed to reveal whether this type of compounds may affect mitochondrial function in intact cells. Although the compounds were chemically and metabolically stable in CEM cell extracts and murine liver homogenates and extensively taken up by intact tumor cells, it is currently still unclear whether these compounds are also able to enter the mitochondrial compartment. Further studies will address this issue, and novel thiourea-substituted β -dThd analogs will be designed to specifically target the mitochondria.

In conclusion, we revealed a new class of compounds that are potent inhibitors of TK-2. They have unusual kinetic properties against TK-2, suggesting specific binding of the inhibitors to an enzyme-ATP complex. This kinetic behavior is in agreement with our computer-assisted molecular modeling results. This type of specific TK-2 inhibitors that do not inhibit cytosolic TK-1 may be useful tools for investigating the mitochondrial depletion syndrome that is caused by (partial) TK-2 deficiency and the role of TK-2 in the homeostasis of the mitochondria. The surprising close correlation between

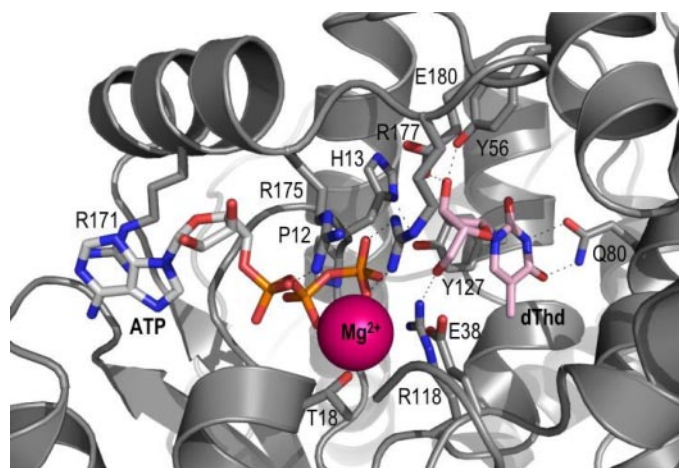


Fig. 6. View of the active site of HSV TK (gray ribbon) as seen in the simulated Michaelis-Menten complex. ATP and dThd are shown as sticks with carbon atoms colored in white and pink, respectively, and Mg^{2+} is displayed as a sphere colored in magenta. Broken lines represent hydrogen bonds between relevant residues discussed in the text.

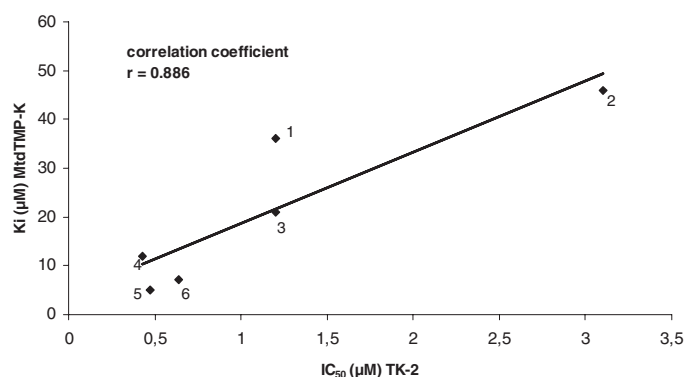


Fig. 7. Correlation between the IC_{50} values of the inhibitors against TK-2 and their K_i values against TMPKmt. The K_i values were taken from Van Daele et al. (2007). The numbering corresponds to the compound numbers depicted in Fig. 1.

the inhibitory activities of the compounds against TK-2 and the distantly related thymidylate kinase of *M. tuberculosis* is strongly indicative for close structural/functional similarities between both enzymes.

Acknowledgments

We highly appreciate the technical assistance of Lizette van Berckelaer and Kristien Minner and the editorial help of Christiane Callebaut.

References

- Allen FH (2002) The Cambridge Structural Database: a quarter of a million crystal structures and rising. *Acta Crystallogr B* **58**:380–388.
- Aqvist J (1990) Ion-water interaction potentials derived from free energy perturbation simulations. *J Phys Chem* **94**:8021–8024.
- Balzarini J, Hernández AI, Roche P, Esnouf R, Karlsson A, Camarasa MJ, and Pérez-Pérez MJ (2003) Non-nucleoside inhibitors of mitochondrial thymidine kinase (TK-2) differentially inhibit the closely related herpes simplex virus type 1 TK and *Drosophila melanogaster* multifunctional deoxynucleoside kinase. *Mol Pharmacol* **63**:263–270.
- Balzarini J, Zhu C, De Clercq E, Pérez-Pérez MJ, Chamorro C, Camarasa MJ, and Karlsson A (2000) Novel ribofuranosyl nucleoside lead compounds for potent and selective inhibitors of mitochondrial thymidine kinase-2. *Biochem J* **351**:167–171.
- Balzarini J, Degrevé B, Zhu C, Durini E, Porcu L, De Clercq E, Karlsson A, and Manfredini S (2001) 2'-O-Acyl/alkyl-substituted arabinosyl nucleosides as inhibitors of human mitochondrial thymidine kinase. *Biochem Pharmacol* **61**:727–732.
- Bayly CI, Cieplak P, Cornell WD, and Kollman PA (1993) A well-behaved electrostatic potential based method using charge-restraints for deriving charges: the RESP model. *J Phys Chem* **97**:10269–10280.
- Case DA, Cheatham TE 3rd, Darden T, Gohlke H, Luo R, Merz KM Jr, Onufriev A, Simmerling C, Wang B, and Woods RJ (2005) The Amber biomolecular simulation programs. *J Comput Chem* **26**:1668–1688.
- Champaness JN, Bennett MS, Wien F, Visse R, Summers WC, Herdewijn P, de Clercq E, Ostrowski T, Jarvest RL, and Sanderson MR (1998) Exploring the active site of herpes simplex virus type-1 thymidine kinase by X-ray crystallography of complexes with acyclovir and other ligands. *Proteins* **32**:350–361.
- Cherrington JM, Allen SJ, McKee BH, and Chen MS (1994) Kinetic analysis of the interaction between the diphosphate of (S)-1-(3-hydroxy-2-phosphonylmethoxypropyl)cytosine, ddCTP, AZTTP, and FIAUTP with human DNA polymerases beta and gamma. *Biochem Pharmacol* **48**:1986–1988.
- Ciliberti N, Manfredini S, Angusti A, Durini E, Solaroli N, Vertuani S, Buzzoni L, Bonache MC, Ben-Shalom E, Karlsson A, et al. (2007) Novel selective human mitochondrial kinase inhibitors: design, synthesis and enzymatic activity. *Bioorg Med Chem* **15**:3065–3081.
- Cornell WD, Cieplak P, Bayly CI, Gould IR, Merz KM, Ferguson DM, Spellmeyer DC, Fox T, Caldwell JW, and Kollman PA (1995) A second generation force field for the simulation of proteins, nucleic acids, and organic molecules. *J Am Chem Soc* **117**:5179–5197.
- Darden TA, York D, and Pedersen L (1993) Particle mesh Ewald: An N-log(N) method for Ewald sums in large systems. *J Chem Phys* **98**:10089–10092.
- Degrevé B, Esnouf R, De Clercq E, and Balzarini J (2000) Selective abolishment of pyrimidine nucleoside kinase activity of herpes simplex virus type 1 thymidine kinase by mutation of alanine-167 to tyrosine. *Mol Pharmacol* **58**:1326–1332.
- Familiar O, Munier-Lehmann H, Negri A, Gago F, Douguet D, Rigouts L, Hernández AI, Camarasa MJ, and Pérez-Pérez MJ (2008) Exploring acyclic nucleoside analogues as inhibitors of Mycobacterium tuberculosis thymidylate kinase. *Chem Med Chem* **3**:1083–1093.
- Fetzer J, Michael M, Bohner T, Hofbauer R, and Folkers G (1994) A fast method for obtaining highly pure recombinant herpes simplex virus type 1 thymidine kinase. *Protein Expr Purif* **5**:432–441.
- Fiser A and Sali A (2003) ModLoop: automated modeling of loops in protein structures. *Bioinformatics* **19**:2500–2501.
- Frisch MJ, Trucks GW, Schlegel HB, Scuseria GE, Robb MA, Cheeseman JR, Zakrzewski VG, Montgomery JA, Stratmann RE, and Burant JC (2003) Gaussian 03, revision 13.04. Gaussian, Inc., Pittsburgh, PA.
- Ghose AK and Crippen GM (1987) Atomic physicochemical parameters for three-dimensional-structure-directed quantitative structure-activity relationships. 2. Modeling dispersive and hydrophobic interactions. *J Chem Inf Comput Sci* **27**:21–35.
- Göbel U, Sander C, Schneider R, and Valencia A (1994) Correlated mutations and residue contacts in proteins. *Proteins* **18**:309–317.
- Hernández AI, Balzarini J, Karlsson A, Camarasa MJ, and Pérez-Pérez MJ (2002) Acyclic nucleoside analogues as novel inhibitors of human mitochondrial thymidine kinase. *J Med Chem* **45**:4254–4263.
- Hernández AI, Balzarini J, Rodríguez-Barrios F, San-Félix A, Karlsson A, Gago F, Camarasa MJ, and Pérez-Pérez MJ (2003) Improving the selectivity of acyclic nucleoside analogues as inhibitors of human mitochondrial thymidine kinase: replacement of a triphenylmethoxy moiety with substituted amines and carboxamides. *Bioorg Med Chem Lett* **13**:3027–3030.
- Hernandez AI, Familiar O, Negri A, Rodríguez-Barrios F, Gago F, Karlsson A, Camarasa MJ, Balzarini J, and Pérez-Pérez MJ (2006) N1-substituted thymine derivatives as mitochondrial thymidine kinase (TK-2) inhibitors. *J Med Chem* **49**:7766–7773.
- Jorgensen WL, Chandrasekhar J, Madura JD, Impey RW, and Klein ML (1983) Comparison of simple potential functions for simulating liquid water. *J Chem Phys* **79**:926–935.
- Kierdaszuk B, Krawiec K, Kazimierzczuk Z, Jacobsson U, Johansson NG, Munch-Petersen B, Eriksson S, and Shugar D (1999) Substrate/inhibitor properties of human deoxycytidine kinase (dCK) and thymidine kinases (TK1 and TK2) towards the sugar moiety of nucleosides, including O'-alkyl analogues. *Nucleosides Nucleotides* **18**:1883–1903.
- Kohler JJ and Lewis W (2007) A brief overview of mechanisms of mitochondrial toxicity from NRTIs. *Environ Mol Mutagen* **48**:166–172.
- Lewis W, Day BJ, and Copeland WC (2003) Mitochondrial toxicity of NRTI antiviral drugs: an integrated cellular perspective. *Nat Rev Drug Discov* **2**:812–822.
- Lim SE and Copeland WC (2001) Differential incorporation and removal of antiviral deoxynucleotides by human DNA polymerase γ . *J Biol Chem* **276**:23616–23623.
- Lupyan D, Leo-Macias A, and Ortiz AR (2005) A new progressive-iterative algorithm for multiple structure alignment. *Bioinformatics* **21**:3255–3263.
- Lynx MD and McKee EE (2006) 3'-Azido-3'-deoxythymidine (AZT) is a competitive inhibitor of thymidine phosphorylation in isolated rat heart and liver mitochondria. *Biochem Pharmacol* **72**:239–243.
- Mancuso M, Salviati L, Sacconi S, Otaegui D, Camaño P, Marina A, Bacman S, Moraes CT, Carlo JR, Garcia M, et al. (2002) Mitochondrial DNA depletion: mutations in thymidine kinase gene with myopathy and SMA. *Neurology* **59**:1197–1202.
- Manfredini S, Baraldi PG, Durini E, Porcu L, Angusti A, Vertuani S, Solaroli N, De Clercq E, Karlsson A, and Balzarini J (2001) Design, synthesis and enzymatic activity of highly selective human mitochondrial thymidine kinase inhibitors. *Bioorg Med Chem Lett* **11**:1329–1332.
- Negri A, Familiar O, Balzarini J, Munier-Lehmann H, Camarasa MJ, Gago F, and Pérez-Pérez MJ (2007) Unexpected similarities between a human and a mycobacterial enzyme that catalyze a different reaction, in Abstracts of the XV Congreso de la Sociedad Española de Química Terapéutica; 2007 Sep 11–14; San Lorenzo de El Escorial, Spain. Poster no. 22.
- Ostermann N, Lavie A, Padiyar S, Brundiers R, Veit T, Reinstein J, Goody RS, Konrad M, and Schlichting I (2000) Potentiating AZT activation: structures of wild-type and mutant human thymidylate kinase suggest reasons for the mutants' improved kinetics with the HIV prodrug metabolite AZTMP. *J Mol Biol* **304**:43–53.
- Pérez-Pérez MJ, Priego EM, Hernández AI, Familiar O, Camarasa MJ, Negri A, Gago F, and Balzarini J (2008) Structure, physiological role, and specific inhibitors of human thymidine kinase 2 (TK2): present and future. *Med Res Rev* **28**:797–820.
- Priego EM, Balzarini J, Karlsson A, Camarasa MJ, and Pérez-Pérez MJ (2004) Non-nucleoside inhibitors of mitochondrial thymidine kinase (TK-2) differentially inhibit the closely related herpes simplex virus type 1 TK and *Drosophila melanogaster* multifunctional deoxynucleoside kinase. *Bioorg Med Chem* **12**:5079–5090.
- Ryckaert JP, Cicotti G, and Berensden HJ (1977) Numerical integration of the cartesian equations of motion of a system with constraints: molecular dynamics of n-alkanes. *J Comput Phys* **23**:327–341.
- Saada A, Shaag A, Mandel H, Nevo Y, Eriksson S, and Elpeleg O (2001) Mutant mitochondrial thymidine kinase in mitochondrial DNA depletion myopathy. *Nat Genet* **29**:342–344.
- Stewart JJ (1990) MOPAC: a semiempirical molecular-orbital program. *J Comput Aided Mol Des* **4**:1–105.
- Van Daele I, Munier-Lehmann H, Froeyen M, Balzarini J, and Van Calenbergh S (2007) Rational design of 5'-thiourea-substituted alpha-thymidine analogues as thymidine monophosphate kinase inhibitors capable of inhibiting mycobacterial growth. *J Med Chem* **50**:5281–5292.
- Viswanadhan VN, Ghose AK, Revankar GR, and Robins RK (1989) Atomic physicochemical parameters for three dimensional structure directed quantitative structure-activity relationships. 4. Additional parameters for hydrophobic and dispersive interactions and their application for an automated superposition of certain naturally occurring nucleoside antibiotics. *J Chem Inf Comput Sci* **29**:163–172.
- Vogt J, Perozzo R, Pautsch A, Protá A, Schelling P, Pilger B, Folkers G, Scapozza L, and Schulz GE (2000) Nucleoside binding site of herpes simplex type 1 thymidine kinase analyzed by X-ray crystallography. *Proteins* **41**:545–553.
- Wild K, Bohner T, Folkers G, and Schulz GE (1997) The structures of thymidine kinase from herpes simplex virus type 1 in complex with substrates and a substrate analogue. *Protein Sci* **6**:2097–2106.

Address correspondence to: Dr. Jan Balzarini, Rega Institute for Medical Research, K. U. Leuven, Minderbroedersstraat 10, B-3000 Leuven, Belgium. E-mail: jan.balzarini@rega.kuleuven.be